

REPORT DOCUMENTATION PAGE

AFRL-SR-AR-TR-04-

Public reporting burden for this collection of information is estimated to average 1 hour per response, including the time for reviewing the data needed, and completing and reviewing the collection of information. Send comments regarding this burden estimate or any other aspect of this collection of information, including suggestions for reducing the burden, to Department of Defense, Washington Headquarters (0704-0188), 1215 Jefferson Davis Highway, Suite 1204, Arlington, VA 22202-4302. Respondents should be aware that any penalty for failing to comply with a collection of information if it does not display a currently valid OMB control number.

0185

| | | | | | |
|--|-------------|--------------------------------|-------------------------------|--|---|
| 1. REPORT DATE (DD-MM-YYYY) | | 2. REPORT TYPE Final Report | | 3. DATES COVERED (From - To) May 1, 01 - Dec 31, 03 | |
| 4. TITLE AND SUBTITLE Center For Digital Security | | | | 5a. CONTRACT NUMBER | |
| | | | | 5b. GRANT NUMBER F49620-01-1-0327 | |
| | | | | 5c. PROGRAM ELEMENT NUMBER | |
| 6. AUTHOR(S) Dr. David M. Roche | | | | 5d. PROJECT NUMBER | |
| | | | | 5e. TASK NUMBER | |
| | | | | 5f. WORK UNIT NUMBER | |
| 7. PERFORMING ORGANIZATION NAME(S) AND ADDRESS(ES) University of California, Davis Office of Sponsored Programs 118 Everson Hall One Shields Avenue Davis, CA 95616-8671 | | | | 8. PERFORMING ORGANIZATION REPORT NUMBER | |
| 9. SPONSORING/MONITORING AGENCY NAME(S) AND ADDRESS(ES) Department of the Air Force Air Force Office of Scientific Research 4015 Wilson Blvd. Arlington, VA 22203-1954 | | | | 10. SPONSOR/MONITOR'S ACRONYM(S) | |
| | | | | 11. SPONSOR/MONITOR'S REPORT NUMBER(S) | |
| 12. DISTRIBUTION/AVAILABILITY STATEMENT Distribution Statement: Approved for public release; distribution unlimited | | | | | |
| 13. SUPPLEMENTARY NOTES DODAAD CODE: Program Manager: Dr. Robert Herklotz | | | | | |
| 14. ABSTRACT Philosophy: The transmission characteristics of optical fibers are of utmost importance for future communication systems. Higher bandwidth and better signal quality are but a few of the reasons that fiber optics are replacing conventional means of communication. However, an optical signal experiences all kinds of losses as it propagates and demands the use of regenerators or repeaters along the length of the fiber. External factors that can cause such losses include deformations of the fiber such as bends or environmental effects such as electrical fields. Consequently, a better understanding of these losses will lead to more efficient optical communication systems. | | | | | |
| 15. SUBJECT TERMS | | | | | |
| 16. SECURITY CLASSIFICATION OF: | | | 17. LIMITATION OF ABSTRACT | 18. NUMBER OF PAGES | 19a. NAME OF RESPONSIBLE PERSON Dr. David M. Roche |
| a. REPORT | b. ABSTRACT | c. THIS PAGE | | | 19b. TELEPHONE NUMBER (Include area code) 530-752-6839 |

20040423 043

David M. Rocke, PI

AFOSR Agreement Number F49620-01-1-0327

**Performance Report Year 3 and
Final Report Years 1-3.**

December 2003

Center for Digital Security
University of California, Davis

Project Title : Modeling Communication Losses and Interference in Fiber Optic Systems

Principal Investigator : Garry Rodrigue

Philosophy : The transmission characteristics of optical fibers are of utmost importance for future communication systems. Higher bandwidth and better signal quality are but a few of the reasons that fiber optics are replacing conventional means of communication. However, an optical signal experiences all kinds of losses as it propagates and demands the use of regenerators or repeaters along the length of the fiber. External factors that can cause such losses include deformations of the fiber such as bends or environmental effects such as electrical fields. Consequently, a better understanding of these losses will lead to more efficient optical communication systems.

Methodology : Numerical simulation is used to study the losses in optical fibers incurred by external factors. The underlying model is the nonlinear vector wave equation

$$\epsilon \frac{\partial^2 \vec{E}}{\partial t^2} = \nabla^2 \vec{E} - \frac{\partial^2 \vec{P}}{\partial t^2}$$

The Galerkin method provides the numerical approximation

$$\tilde{E}(\vec{x}, t) = \sum_{j=1}^N e_j(t) \vec{W}(\vec{x})$$

where $\vec{W}_1, \vec{W}_2, \dots, \vec{W}_N$ are vector polynomials. Propagating modes that satisfy the above nonlinear wave equation must be tangentially continuous across interfaces. Hence, numerical approximations must do the same as is accomplished by using Whitney edge elements as the vector polynomial basis functions \vec{W}_i .

Accomplishments (2003) :

Bent Step-Indexed Fibers

The indices of refraction in a straight step-indexed optical fiber govern the type of light waves that will be guided. However, if the fiber is bent, the guidance properties of the fiber no longer hold and the optical wave may leak out of the fiber core into the cladding resulting in premature wave attenuation. Figure 1(a) illustrates the 1.8 million element approximation of

a 52.8 micron length of a bent fiber with 55.13 micron bend radius. 5.66 million unknowns are required to be numerically determined. The computation requires 72 hours on 38 processors of the Maui High Performance Computing Center (MHPCC) Huinalu Linux based supercomputer and 22 hours on 38 processors of the LLNL MCR Linux based supercomputer. The Gaussian pulse of the TE_{01} mode can be seen in Figure 1(b) where the core is purple and the cladding green. A close-up of the pulse interacting with core-cladding interface is shown in Figure 1(c) where the core is again purple and the cladding is blue. The power of the optical wave at the end of the bend was measured to be 109 W/m in contrast to the power of the wave in a straight fiber which was measured at 522 W/m.

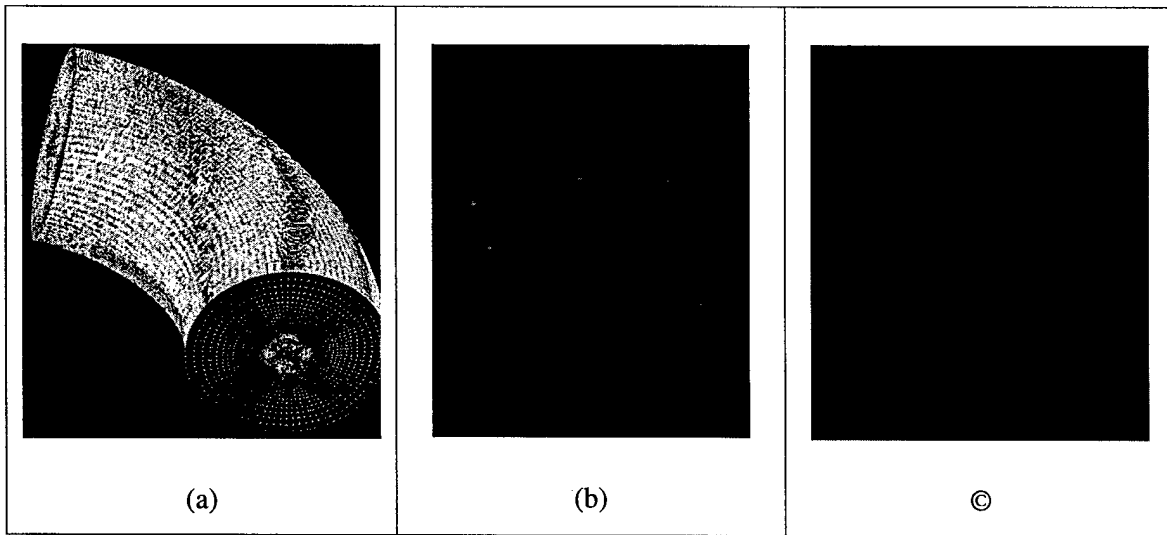


Figure 1 (a) Numerical grid of bent fiber. (b) Leakage of transverse Gaussian pulse. (c) Close-up of leakage

External Microwave Effects :

We study the effect on the propagation of an optical by the external impingement of a highly intense microwave on a step-indexed fiber. The intensity of the microwave is such that a change in the refractive index of the fiber occurs (the Kerr effect). Specifically, the refractive index is described by the relation

$$n = n_0 + 2n_2 |\vec{E}|^2$$

where n_0 represents the usual refractive index and n_2 is a new optical constant that gives the rate at which the refractive index increases with

increasing intensity. Figure 2 illustrates a plane microwave impinging on an optical fiber from the top at 3 sec. and continuing on for another 10 sec. before being terminated. The pulse is left to interact with the propagating guided wave.

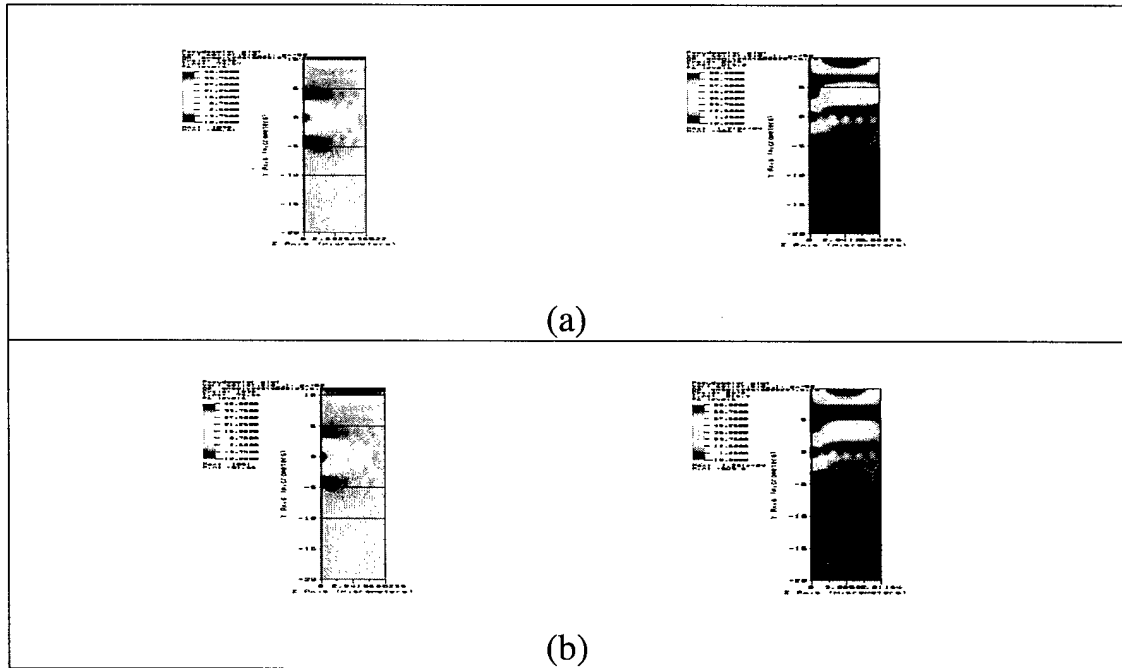


Figure 2. Plot of z-component of optical field. (a) Without Kerr effects. (b) With Kerr effects.

High Order Vector Elements

Simulations on more complicated fibers will require orders of magnitude more elements to represent the geometries and subsequently longer computer run times. Vector basis functions using higher order polynomials instead of the standard Whitney edge elements provide a possible means for reducing the number of elements while maintaining the same accuracy of the computed solutions. Figure 3 illustrates a plot of a typical high order polynomial basis function.

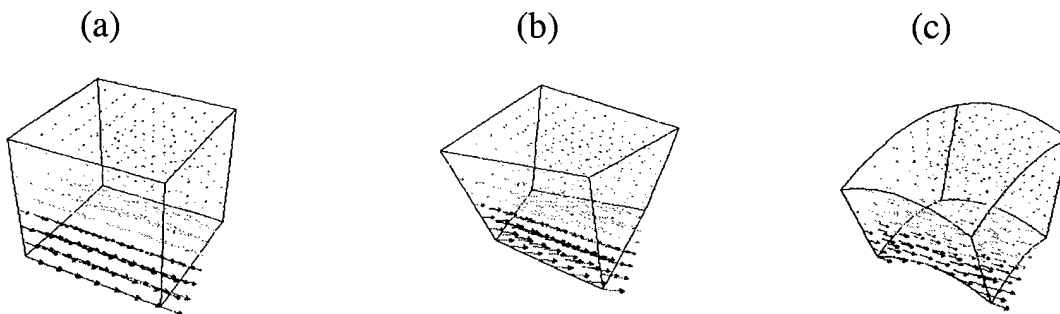


Figure 3. Example of vector polynomial basis function (a) Linear, (b) Quadratic, (c) Cubic

We use the high order elements to compute the modes of a resonant cavity to determine if the same accuracy can be obtained with fewer elements.

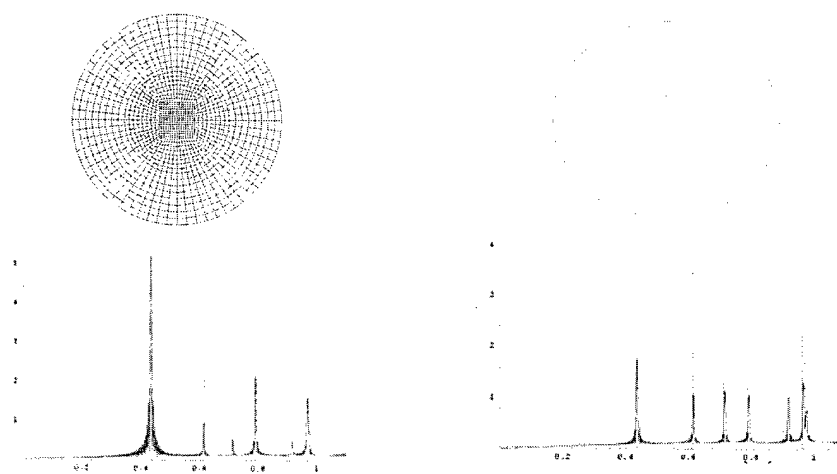


Figure 4. Resonant modes using linear polynomials (a) and (b) cubic polynomials

Figure 4 illustrates the grids used by linear polynomial basis functions and cubic polynomial basis functions. Note the same accuracy for the modes is achieved. The compute time for the linear polynomials was 417 min. and for the cubic polynomials was 11 min. .

IV Mass Lumping :

The inversion of the mass matrix $\mathbf{matrix}[\vec{w}_i \vec{w}_j]$ at every time step of the computation is extraordinarily expensive and impedes simulations of optical propagation over long time intervals. This is due to the fact that the mass matrix is in general non-sparse (see Figure 5).

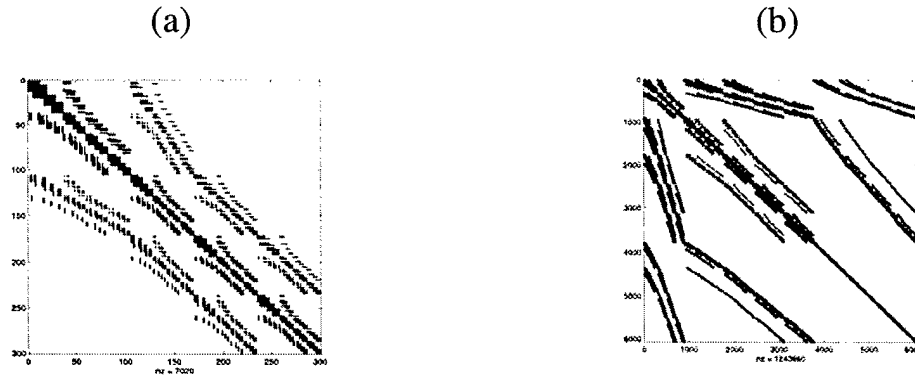


Figure 5. Sparsity pattern of mass matrix for (a) linear vector polynomials and (b) cubic vector polynomials

A new vector polynomial basis has been developed which upon the use of the Gauss-Lobatto quadrature rule yields a block diagonal mass matrix.

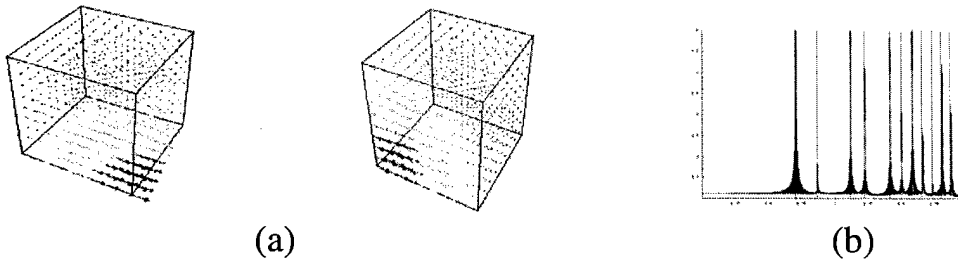


Figure 6. (a) Examples of new linear vector polynomial basis functions. (b) Computed resonant modes on rectangular cavity.

Figure 6 illustrates examples of the new basis functions. They were used to compute up to second order accuracy the resonant modes of a rectangular cavity. This computation was 10 times faster than the computation using the standard Whitney edge element.

Publications :

1 Numerical Studies of Fiber Optical Signal Attenuation from Compression and External Fields, with J. Mariani and J. Koning, Proc. of 2003 MHPCC Application Briefs

2 Arbitrary Order Hierarchical Vector Bases for Hexahedrons, with R. Rieben and D. White, Proc. of IEEE Ant. and Prop. Soc., Columbus, OH, June 22-27, 2003

3 Generalized High Order Interpolatory and Hierarchical Finite Element Vector Bases, with R. Rieben and D. White, accepted for publication IEEE Transactions on Antennas and Propagation

4 Solving the Eikonal Equation on an Adaptive Mesh, with P. Covello, submitted for publication, J. Applied Computational Mathematics

5 Modeling Losses and Interference in Fiber Optic Systems, with P. Covello, J. Koning, and J. Mariani, Proc. Of 2003 AMOS Tech. Conference, Wailea, HI, Sept. 8-13, 2003

Personnel Supported :

Paul Covello, graduate student

Jennifer Mariani, post graduate researcher

CDS

Network Interdiction Project 2002-2003

Personnel:

Prof. David L. Woodruff, Ph.D.

02-03 Harald Held, Dipl. Math

Recent Advances:

We are exploring optimized interdiction of networks where either the characteristics of the network itself or the effect of interdiction efforts cannot be known with certainty in advance. These models add important realism for computer, terrorist or drug transportation networks where the characteristics of the network or the interdiction cannot be known completely in advance but rather interdiction must be planned based on conjectured configurations. In some multi-stage formulations, we model the fact that attacking the network may result in resolving some of the uncertainty. This is particularly relevant for communication and computer networks, but also has relevance for transportation or terrorist networks.

We have developed models and solution methods that are effective. Recently, we have teamed up with R. Kevin Wood of the Naval Postgraduate School to explore new solution methods. We have developed methods that are by far the fastest for these novel, but realistic problem formulations.

Plan for Future Work:

We will proceed on two fronts:

1. We have recently begun to test the methods on realistic computer and transportation networks. This work will continue.
2. We are developing methods that can solve these problems in seconds. This is obviously valuable when the methods are used in a decision support system (DSS) for planning attacks. This is perhaps even more important when used in a DSS to plan defense, since the interdiction problems must be solved repeatedly.

Paper Published in October 2002:

"Interdicting Stochastic Networks with Binary Interdiction Effort," with R. Schultz and R. Hemmecke in D.L. Woodruff (Ed.) *Network Interdiction and Stochastic Integer Programming*, Kluwer Academic Press, 69-84, 2003.

We provide formulations, test instances and benchmark results for a new class of network interdiction problems. The formulations are appropriate for computer, terrorist or drug transportation networks where the characteristics of the network cannot be known completely in advance but rather interdiction must be planned based on conjectured configurations. The models support maximization of the expected minimum path length between two nodes, s and t . We also model maximizing the probability of causing the minimum path length to be above a specified threshold. Examples make our formulations concrete and benchmarks establish the computational requirements for solution. Our benchmarks also help quantify the importance of using a special formulation provided for instances when a cut between s and t is the goal.

Papers Submitted:

1. Held, H, R. Hemmecke, and D.L. Woodruff, "A Decomposition Algorithm for Planning the Interdiction of Stochastic Networks," submitted to *Naval Research Logistics*.

We describe a decomposition based solution method for a new, important class of network interdiction problems. The problem of maximizing the probability of sufficient disruption of the flow of information or goods in a network whose characteristics are not certain is shown to be solved effectively by applying a scenario decomposition method developed by Schultz. Computational results demonstrate the effectiveness of the algorithm and design decisions that result in speed improvements.

2. Held, H. and Woodruff, D.L., "Multi-stage Interdiction of Stochastic Networks," submitted to *Journal of Heuristics*.

We describe and compare heuristic solution methods for a multi-stage stochastic network interdiction problem. The problem is to maximize the probability of sufficient disruption of the flow of information or goods in a network whose characteristics are not certain.

In this formulation, interdiction subject to a budget constraint is followed by operation of the network, which is then followed by a second interdiction subject to a second budget constraint. Computational results demonstrate and compare the effectiveness of heuristic algorithms.

Edited Volume Was Published in Late October 2003:

Network Interdiction and Stochastic Integer Programming, Kluwer Academic Press, 2003.

Each chapter represents state-of-the-art research and all of them were refereed by leading investigators in the respective fields. Problems associated with protecting and attacking computer, transportation, and social networks gain importance as the world becomes more dependent on interconnected systems. Optimization models that address the stochastic nature of these problems are an important part of the research agenda. This work relies on recent efforts to provide methods for addressing stochastic mixed integer programs. The book is organized with interdiction papers first and the stochastic programming papers in the second part. A nice overview of the papers is provided in the Foreward written by Roger Wets.

List of Authors:

Ahmet Balcioglu Naval Postgraduate School

Carl Burch College of St Benedict and St John's University

Robert Carr Sandia National Laboratories

William S. Charlton The University of Texas at Austin

Raymond Hemmecke University of California, Davis

LOW DETECTABILITY OPTICAL CODE-DIVISION MULTIPLE ACCESS COMMUNICATIONS ON A BROADBAND WDM NETWORK.

Professor Brian H. Kolner, Department of Applied Science

This year saw tremendous progress in the development of a prototype Optical Code-Division Multiple Access (OCDMA) fiber-optic communications system. The goal of this system is to allow multiple users to share the same optical fiber and overlap in physical space (spatial modes), time, and wavelength. The current and projected future optical fiber telecommunications systems will depend on dense wavelength-division multiplexing (DWDM) to achieve efficient use of the vast bandwidth available in optical fibers. The International Telecommunications Union (ITU) has standardized the channel spacing and wavelength location around the low-loss region of silica-based optical fiber at 1550 nm. In the current DWDM standard, the channels are spaced at 100 GHz intervals and the fiber and amplifier properties allow for a total of 45 channels or, equivalently, over 1 terahertz of bandwidth (one assumes here that there must be guard bands between each channel boundary to ensure that data does not spill over into adjacent channels).

The OCDMA twist on the DWDM fiber standard provides a method for encoding the data in a manner similar to that used in spread-spectrum technology. Our approach, however, does the encoding in the wavelength, or frequency, domain. Starting with picosecond pulses from a modelocked fiber laser, the spectrum is spread out in space with a diffraction grating and collimated into a parallel and highly elliptical beam. In this beam is placed a liquid crystal phase modulator with 128 individually addressable pixels. The phase of each pixel can be varied continuously from 0 to 2π radians. This accomplishes the encoding of the bit. In a two-level coding scheme there are 2^{128} possible combinations. After passing through the encoding phase modulator the pulse spectrum is brought back together into a round beam with another grating and launched into a fiber. The effect of the coding on the pulse is to dramatically stretch it in time and thus lower its peak power by a commensurate amount. We refer to this as Spectral Phase-Encoded Time Spreading (SPECTS). At the receiver, an identical grating-phase modulator-grating arrangement is used as a decoder. The incoming time-stretched pulses have the same spectral distribution but since the phase across the spectrum has been modified by the encoder, the opposite or conjugate phase must be applied to the decoder in order to reconstruct a transform-limited pulse. Since there are 2^{128} possible combinations of phase codes, the receiver must know, *a priori*, the correct wavelength-domain phase code. This allows for a high degree of security in this communications system. Having many different users share the channel increases the effectiveness, to a point, since the arrival of many different and undecoded pulses creates a background noise layer in which the desired bits can hide.

Although we can use the full 128 bits of our wavelength-domain phase modulator, communications theory tells us that only a small subset of the possible combinations will

form a robust code. By this we mean a code with desirable correlation properties that can give a high degree of discrimination between properly decoded and interfering signals. Thus we have focused on using so-called M-sequence and Walsh codes in our initial simulations of channel effectiveness. These are 31-bit codes that utilize 4 pixels per bit on the modulator. Simulations of bit-error-rate effectiveness by colleagues in the Electrical and Computer Engineering Department have shown that the M-sequence codes produce superior results.

The first major experimental results in the OCDMA program came about with our optical test bed. The purpose of the test bed is to demonstrate the principles of OCDMA and test various coding schemes before launching into the next phase in which we integrate most of the components into indium phosphide technology. The experimental setup is shown in Fig. 1. The mode-locked fiber laser (optical clock) generates 2.4 ps pulses centered at 1550 nm with a repetition rate of 10 GHz. A synchronized LiNbO₃ Mach-Zehnder modulator modulates the pulse train at 10 GHz with a $2^{23} - 1$ pseudo-random bit sequence (PRBS). The modulated pulses are amplified by an Erbium-doped fiber amplifier (EDFA), and then compressed to 0.4 ps by a nonlinear-fiber-based pulse compressor. This pulse train is spectrally phase encoded by a SPECTS pulse shaper and is then decoded by an identical pulse shaper, followed by a threshold detection system composed of a dispersion compensated EDFA and 500 m of highly nonlinear fiber (HNLF). Bit error rate testing was performed using a 10 Gb/s receiver with clock recovery and a HP 70843B test set.

The inset in Fig.1 shows the details of the SPECTS encoder/decoder. A spatial light phase modulator (SLM) is located in the Fourier plane of a zero dispersion pulse compressor consisting of a pair of diffraction gratings and lenses. This arrangement allows the individual spectral components to be phase modulated (0 or π phase shift) by the SLM with an M-sequence code.

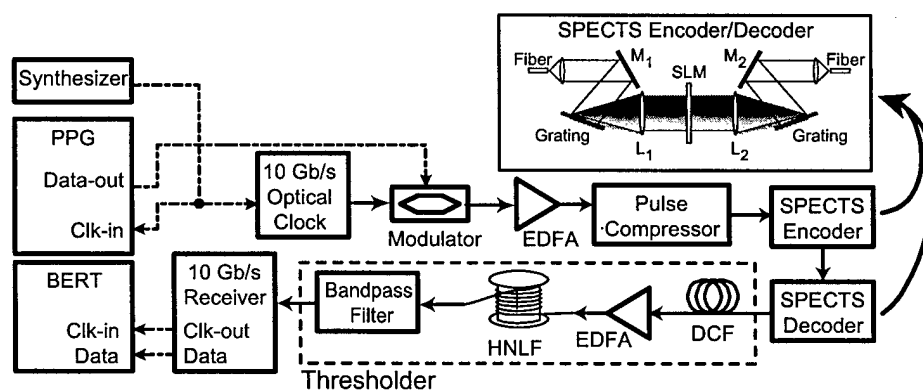


Fig. 1. Diagram of experimental setup for Bit-Error-Rate measurement of SPECTS O-CDMA testbed. BERT; Bit-Error-Rate Tester, PPG; Pulse Pattern Generator, EDFA; Erbium Doped Fiber Amplifier, DCF; Dispersion Compensation Fiber, HNLF, Highly Nonlinear Fiber, SLM; Spatial Light Modulator, L1 & L2; Lenses, M1 & M2; Mirrors.

To verify the proper operation of the encoder and decoder, we made intensity cross-correlation measurements at several key locations in the system (Fig.2). Notice that the

correctly decoded pulse is only slightly broadened when compared with the input pulse (Fig. 2a). While the encoded (Fig. 2b) or incorrectly decoded pulse (Fig. 2c) is broadened approximately 30 times.

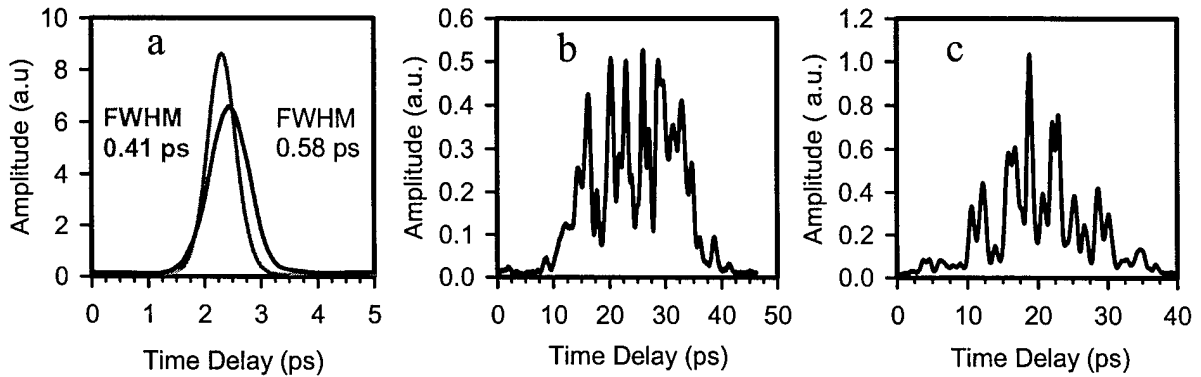


Fig. 2. Cross correlation traces (using 0.4 ps pulse as the reference) showing the optical pulse state at various points in the system. (a) Input pulse to the encoder (gray) and decoder output pulse (black). (b) Encoded pulse with a 31 bit m-sequence on the SLM of encoder. (c) Incorrectly decoded output pulse from the decoder.

Even though the incorrectly decoded pulse is very broad, it will be interpreted the same as the short pulse in typical optical receivers because of their broad temporal response. This mandates the use of a threshold detector which acts as a discriminator. Our approach to threshold detection takes advantage of fiber non-linearity which generates additional frequency components through self-phase modulation for shorter (higher peak power) pulses but not for longer ones. Figure 3a shows the input spectrum to the encoder and the decoder output spectrum. The narrowing of the output spectrum is caused by spectral windowing from the SLM. After passing through the HNLF, the spectrum is significantly broadened (Fig.3b) with the properly decoded pulse showing significantly more spectrum at the longer wavelength when compared to the improperly decoded pulse (rejected) spectrum. When a 1 nm bandpass filter is used at 1561 nm, we measured contrast ratios in excess of 7 dB. Figure 3c shows the output spectra from the thresholder for correctly and incorrectly decoded pulses.

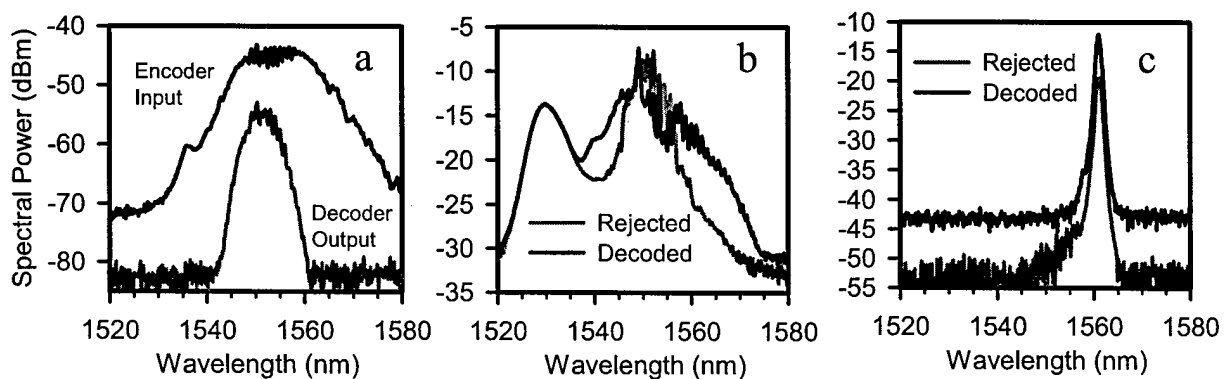


Fig. 3. Optical spectra at various locations in the system. (a) The encoder input spectrum and the decoder output spectrum. (b) Output spectra of the 500 m long HNLF for correctly and incorrectly decoded pulses. (c) Output spectra of the thresholder for correctly and incorrectly decoded pulses.

Quantitative analysis of the performance of any digital communications system is based on the bit-error-rate (BER) test. Fig. 4 shows the bit-error-rates for the system without the CDMA encoder/decoder (back-to-back signal) and the correctly decoded signal that passes through the HNLF-based threshold. The inset shows the eye diagrams of back-to-back, correctly decoded, and incorrectly decoded signals. It clearly shows that the eye diagram of the correctly decoded signal is open widely while the eye of the incorrectly decoded signal is completely closed. The degradation of the incorrectly decoded signal prevents synchronization for a BER measurement at the available powers. In contrast, less than 10^{-11} BER was achieved with a correctly decoded signal. The BER of the incorrectly decoded signal is around 0.4 due to the failure of synchronization while the BER of correctly decoded signal below 10^{-11} .

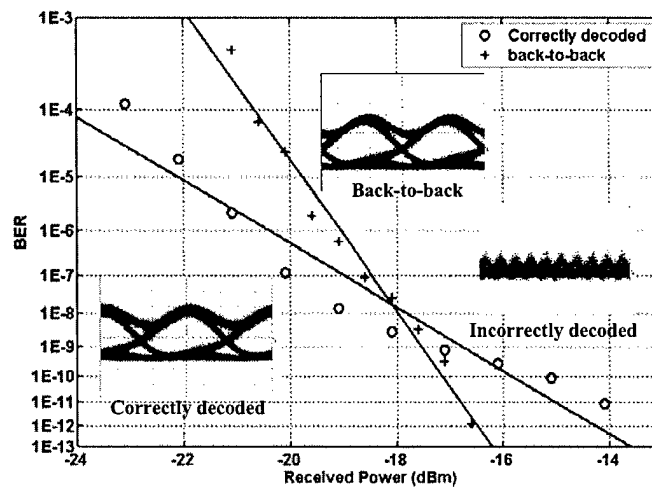


Fig. 4. Bit Error Rate and eye diagrams for back-to-back and decoded signals

These data were collected and submitted for presentation at OFC (Optical Fiber Conference) 2004, which is the most significant forum for research results in fiber optic telecommunications.¹ We are currently working to improve the system performance and will submit the results to an archival journal.

The next step in the OCDMA program is to introduce multiple interferers into the network and study the robustness to variations of the M-sequence codes amongst the interfering signals. In parallel with this effort, we are now fabricating arrayed waveguide gratings and integrated phase modulators in indium phosphide as necessary steps toward realization of an all-integrated OCDMA system.

References:

1. Kebin Li, Wei Cong, V. J. Hernandez, Ryan P. Scott, Jing Cao, Yixue Du, J. P. Heritage, Brian H. Kolner, and S. J. B. Yoo, "10 Gbit/s optical CDMA encoder-decoder BER performance using HNLF threshold," Submitted to the 2004 OFC Conference.

Budget

| Budget Report for AFOSR01 | | | |
|----------------------------------|--------------|-------------|--------------|
| | Budget | Re-Budget | Actual |
| Salaries | \$ 748,777 | \$ (43,112) | \$ 705,665 |
| Benefits | \$ 195,925 | \$ (47,871) | \$ 148,054 |
| Supplies and Expense | \$ 66,095 | \$ (7,369) | \$ 58,726 |
| Equipment | \$ 30,000 | \$ 108,504 | \$ 138,504 |
| Travel | \$ 35,800 | \$ (10,151) | \$ 25,649 |
| Indirect Cost | \$ 423,403 | \$ 0 | \$ 423,403 |
| Total | \$ 1,500,000 | \$ - | \$ 1,500,000 |

Budget Notes: The major change from the original budget was to provide funding for a 32-processor rack-mount Linux cluster for the computational components of the project. We had hoped to provide this capability from a separate DOD equipment proposal, but unfortunately that effort was unsuccessful.